APPLICATION OF AIRBORNE INFRARED TECHNOLOGY TO MONITOR BUILDING HEAT LOSS

Fred J. Tanis
Robert E. Sampson

Infrared and Optics Division
Environmental Research Institute of Michigan

SUMMARY

During the 1975-76 winter heating season ERIM conducted studies to test the application of airborne infrared technology to the requirements for energy conservation in buildings. Quantitative airborne data of the City of Ypsilanti, Michigan were collected and processed to identify roof temperatures. A thermal scanner was flown at an altitude of 1,200 feet with two thermal bands 8.2-9.3 μm and 10.4-12.5 μm recorded by an analog system. Calibration was achieved by standard hot and cold plates. Using a thermal model to interpret ceiling insulation status, environmental factors were found to influence the relation between roof temperature and insulation. These include interior and sky temperatures, roofing materials, and the pitch and orientation of the roof. A follow-up mail survey established the ability to identify insulated and uninsulated houses from the airborne infrared data.

INTRODUCTION

Increasing costs of energy have led to major reexamination of procedures for insulation, and maintenance of existing buildings. As part of this reanalysis, the Environmental Research Institute of Michigan (ERIM) has investigated the use of an aerial thermal scanner system to evaluate building insulation characteristics [1].

Alternatives available for determining the adequacy of building insulation within a community are limited. Fuel use data is difficult to interpret and lack of knowledge about insulation and number of buildings within a community makes direct survey techniques impractical. In addition, actual presence of insulation within a building is often not a true indication of its adequacy. Defective insulation, setting, and aging result in significant changes in thermal transmission properties. Thus, a method is sought which will rapidly yield heat-loss information about large numbers of buildings in order to identify effective insulation characteristics as well as roof areas with critical heat loss. Some aerial infrared survey work of cities have been conducted such as the study performed by CENGAS, a Nebraska gas utility, in February 1975 [2]. These surveys produced black and white photographic images which were largely qualitatively interpreted. The methodology employed in the present study used a one-dimensional heat transfer model of a gable roof system to aid the interpretation of results.

AERIAL THERMAL IMAGERY

Aerial thermal imagery was collected using the thermal IR channels of ERIM's 12-channel multispectral scanner system. The two thermal bands simultaneously recorded were in the 8.2-9.3 μm and the 10.4-12.5 μm wavelength ranges. A visible band was also recorded but because the data were recorded at night only street lights and building exterior lights were recorded.

The two cryogenically cooled radioation detectors were digitized and recorded on magnetic tape for later playback. The scanner optics record two temperature reference plates internal to the scanner. There reference plates were maintained at carefully controlled temperatures for later temperature calibration of the thermal imagery. A 70 mm film strip print was produced from a continuous tone video image. Because these data are initially recorded on magnetic tape, electronic editing, calibration, and enhancement procedures can provide a number of possible final image products.

The airborne thermal survey was completed during the evening of November 23, 1975. Surface temperature was reported to be -5°C with a wind speed of 3 knots/hour. Flight data was obtained near midnight under clear sky conditions. The flight data consisted of three-four mile flight lines over Ypsilanti and two-three mile flight lines over Ann Arbor at an altitude of 1,200 feet. A map of the area covered is shown in Figure 1.

Aerial data were interpreted using two types of imagery -- continuous tone images indicating relative temperature differences by variations in contrast (or graytone) and black and white temperature "slices". Examples of these two types of imagery are shown in Figure 2.

To produce the calibrated "slices", the aerial data were quantized into discrete signal levels representing 16 "apparent" temperature ranges from 10° to 40°F. These were individually images and photographed such that all portions of the scene having the same temperature range were highlighted, while all surface temperatures outside that range appear black. Thus, 16 black and white strip-prints provide quantitative evidence of building roof temperatures and their variations. By producing a series of these temperature slices, each with a different increment, the full temperature range of the scene is represented. Surface water and vegetated areas generally are warmer than the roof surfaces. Roof temperatures are generally colder than air temperatures on clear nights due to the net transfer of heat by radiation to the cold sky.

It must be noted that these are "apparent" temperatures. For most surfaces the emissivity is 0.8 or greater, for asphalt shingles a value of 0.91 is acceptable. Part of the observed radiance is a reflection of the cold sky. The radiance temperature of the cold sky was assumed to be -30°C for the clear sky conditions that prevailed at the time of the flight. The reflectivity of the roof surfaces, which is equal to one minus the emissivity, was taken to be 0.09. Under these set of circumstances, the actual roof surface temperatures were 2 to 3°C warmer than the "apparent" temperature slices indicated.

MODEL DEVELOPMENT

A one dimensional model of the roof heat loss was developed to interpret the observed roof temperatures from the flight data. Heat loss through a ceiling and gabled roof system can be simulated by four equations which are expressions of the first law of thermo-dynamics for the roof exterior surface, roof interior surface, attic air, and ceiling. All calculations were made with environmental parameters determined by conditions as they occurred during the time of the aerial flight.

Model calculations were made in three steps:

1) Apparent roof temperatures, as determined from the aerial imagery were converted to actual roof temperatures by calculating the effect of roof emissivities.

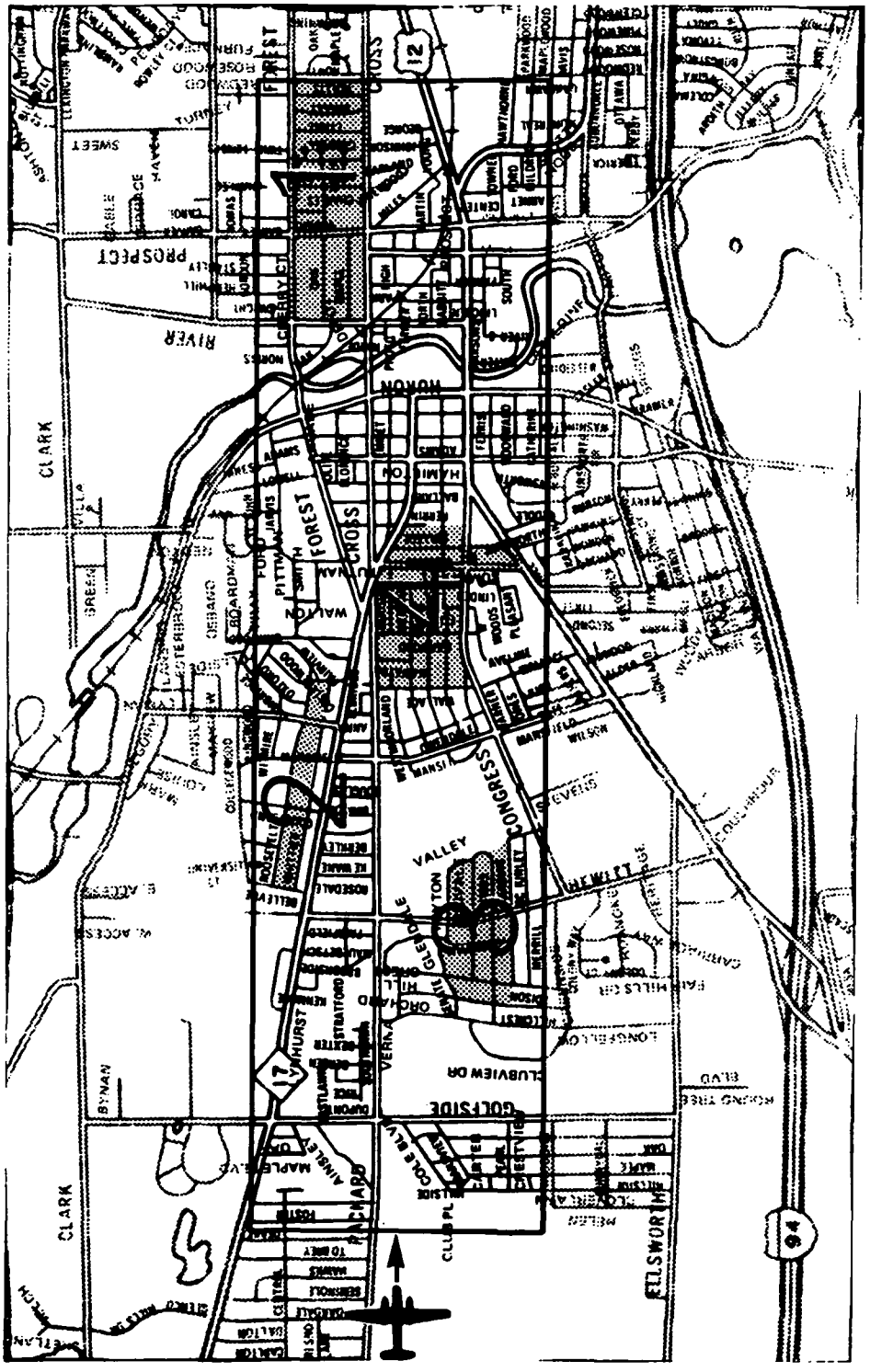

FIGURE 1. CITY OF YPSILANTI WITH OUTLINE OF FLIGHT COVERAGE AND GROUND SURVEYED SUBAREAS

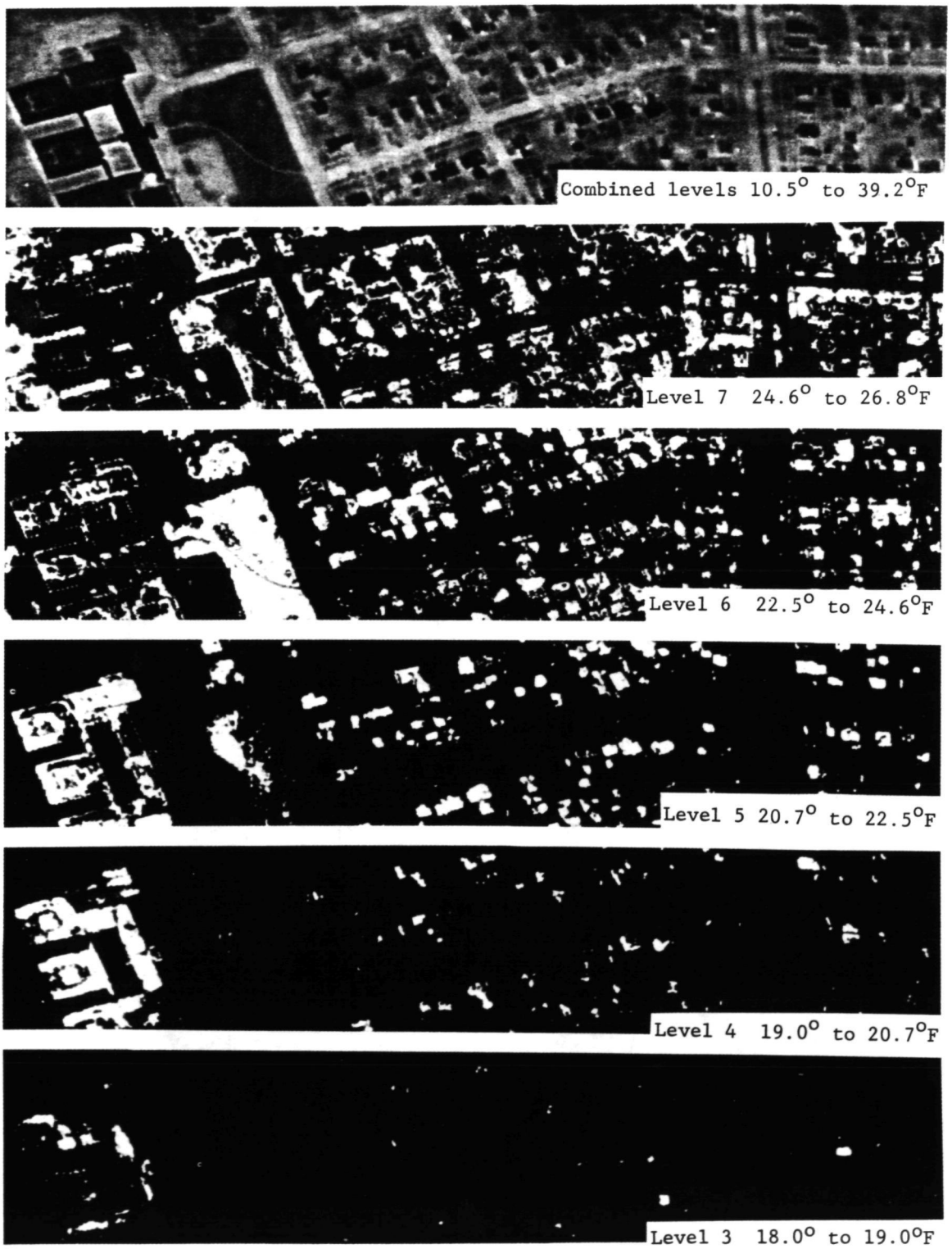

FIGURE 2. CALIBRATED THERMAL IMAGERY OF YPSILANTI, MICHIGAN. Full range plus temperature slices. (bandwidth 10.4-12.5 μm)

2) Heat loss from a simulated roof was determined as a function of the roof temperature.

3) Three equations describing heat balance through the ceiling, the roof, and the attic vents were solved for the ceiling transmission (U) factor (see the diagram in Figure 3).

The equations, for roof heat loss are sensitive to surface emissivities, roof view factors, and the temperatures which determine radiation gains from the physical surroundings and from the ambient air. Radiation energy exchange rates are generally larger than the convective energy exchange in the roof temperature range of interest.

Buildings recorded in the aerial survey which have pitched rather than flat roofs, receive radiation from nearby surrounding surfaces such as adjacent trees and buildings. The total view factor, comprised of areas of sky and surroundings, must add to unity. Thus, the view factor represented by surrounding surfaces is that fraction of the total roof exposure which is occupied by trees, buildings, poles, and other terrestrial features.

The residential flight data included both new and old neighborhoods. Most of the newer homes were oriented with their roof lines parallel to the adjacent streets, and the trees were generally small. Roof pitches tend to be 4/12 to 5/12. On the other hand, many of the older Ypsilanti houses have much greater pitches (8/12 or 10/12) and the roof lines are perpendicular to the street direction. These areas also have larger trees. These older houses are situated on small lots offering greater exposure to one another. For the low pitch roofs, the entire roof is assumed to be exposed to only objects above the horizon. In this case, the view factor (F_{VS}) for the surroundings is calculated to be 0.125. For high pitched roofs (10/12), the eaves of one roof are looking up at the peak of the next house. The peak is receiving radiation from surfaces below the horizon. The maximum angle of incidence for the roof is about 40° at the peak and 60° at the eaves. An average view factor was calculated to be 0.28 for a 10/12 pitched roof.

The value of the heat loss through the roof is used to estimate the temperature T_i just inside the roof by:

$$U_r (T_i - T_r) = \epsilon_r \sigma T_r^4 - \epsilon_r \epsilon_\infty F_\infty \sigma T^4 - \epsilon_r \epsilon_s F_s \sigma T_s^4 - h_c (T_\infty - T_r) \quad (1)$$

where

U_r is the combined heat transfer conductance of the roof

T_i is inside roof temperature

ϵ_r is roof emissivity

σ is Stefan-Boltzmann constant

ϵ_∞ is ambient air emissivity

F_∞ is ambient air view factor

T_∞ is ambient air temperature

ϵ_s is emissivity of surroundings other than ambient air

F_s is view factor to surroundings

T_s is surrounding temperature

h_c is convective coefficient on the roof surface

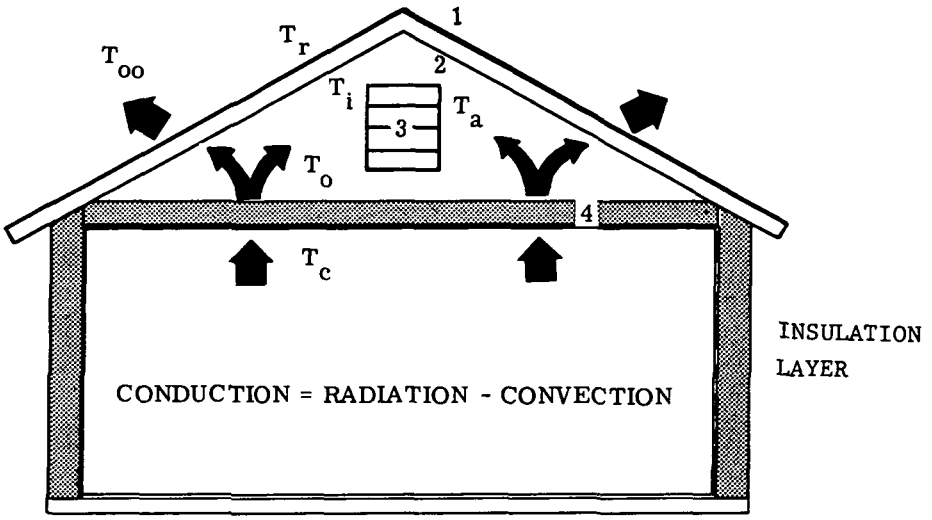

FIGURE 3. DIAGRAM FOR ONE DIMENSIONAL THERMAL MODEL OF HEAT LOSS FOR A GABLED HOUSE.

This equation can be solved directly for T_i, the inside roof temperature assuming T_r is measured by infrared instrumentation.

The transmission coefficient used for the uninsulated roof structure was 0.885. This coefficient represents a roof constructed of a half inch of plywood, a layer of building felt, and a covering of asphalt shingles.

Values of T_i were substituted into the remaining three heat balance equations below and solved for the transmission, U-factor, of the ceiling. Since the equations are non-linear in temperature, the solution is obtained by iteration.

$$U_r (T_i - T_r) = \frac{\sigma T_o^4 - \sigma T_i^4}{\frac{\rho_o}{\epsilon_o} + \frac{\rho_i}{\epsilon_i}\left(\frac{A_i}{A_o}\right) + 1} + h_i (T_a - T_i) \qquad (2)$$

where

T_o is attic floor temperature

ρ_o is attic floor reflectivity

ϵ_o is attic floor emissivity

ρ_i is inside roof reflectivity

ϵ_i is inside roof emissivity

$\frac{A_i}{A_o}$ is ratio of inside roof area to attic floor area

h_i is the convective coefficient on the inside of the roof

T_a is attic air temperature

$$h_o (T_o - T_a) = h_i (T_a - T_i) + \frac{A_e}{A_o} U_e (T_a - T_\infty) + q_v \qquad (3)$$

where

h_o is heat transfer coefficient on the floor of the attic

$\frac{A_e}{A_o}$ is the ratio of the wall area at the ends of the attic to the attic floor area

U_e is the combined heat transfer conductance of the attic end

q_v is the energy flow out of the vents = $m' Cp (T_a - T_\infty)$

where

m' is mass flow rate based on wind speed and direction or buoyancy force and

Cp is specific heat.

$$U_o (T_c - T_o) = h_o (T_o - T_a) + \frac{\sigma T_o^4 - \sigma T_i^4}{\frac{\rho_o}{\epsilon_o} + \frac{\rho_i}{\epsilon_i}\left(\frac{A_i}{A_o}\right)+1} \quad (4)$$

where T_c is inside ceiling temperature and U_c is ceiling conductance.

RESULTS

Solutions to the heat balance equations are shown in Figures 4 and 5 as graphs of roof temperature versus the ceiling U-transmission factor and heat loss for the 5/12 and the 10/12 gabled roof construction. The temperatures which correspond to the numbered temperature "slices" produced from the aerial data are also shown on these figures. The model indicates that the upper and lower bounds of the temperatures under the weather conditions for the time of flight should be slice 3 (15°F) and slice 8 (28°F). Nearly all roof temperatures from the aerial thermal imagery lie in this range. The few exceptions may be due to special roofing materials which have unusually low emissive properties. Varying the inside (T_C) and outside (T_{oo}) air temperatures indicate that the above roof temperatures would shift directly with changes in the ambient air temperature, but only slightly with changes in inside temperature.

The model results suggest that knowledge of roof pitch and structure are required to distinguish the amount of ceiling insulation or its equivalent resistance. However, clearly it should be possible to distinguish houses with little or no insulation from those which are well insulated. For this example, temperature level six (23°F) would be the optimum detection boundary for inadequate insulated roof systems.

Questionnaires were sent to approximately one thousand homes located in the four subareas to check the results of the analysis. The questionnaire requested that residences estimate the amount of ceiling insulation in their homes. The responses were compared to the results of the analysis by identifying individual roof temperature.

These survey results which are summarized in Table 1, are positive and relate well to the model studies. While there was too much variation to use the observed roof temperatures to predict precise amounts of insulation, it was possible to interpret thermal aerial imagery for purposes of identifying insulated and non-insulated houses. Using a 5 and 6 level discriminant Figure 6 shows percent correct classification as a function of temperature level.

Gas consumption values were estimated at the time of overflight from data provided by the local utility. Consumption values increase with the poorer insulation conditions but exhibit a large amount of scatter with ceiling insulation undoubtedly due to variability in the house size, interior temperatures, sidewall losses and infiltration losses. Figure 7 shows the distribution of

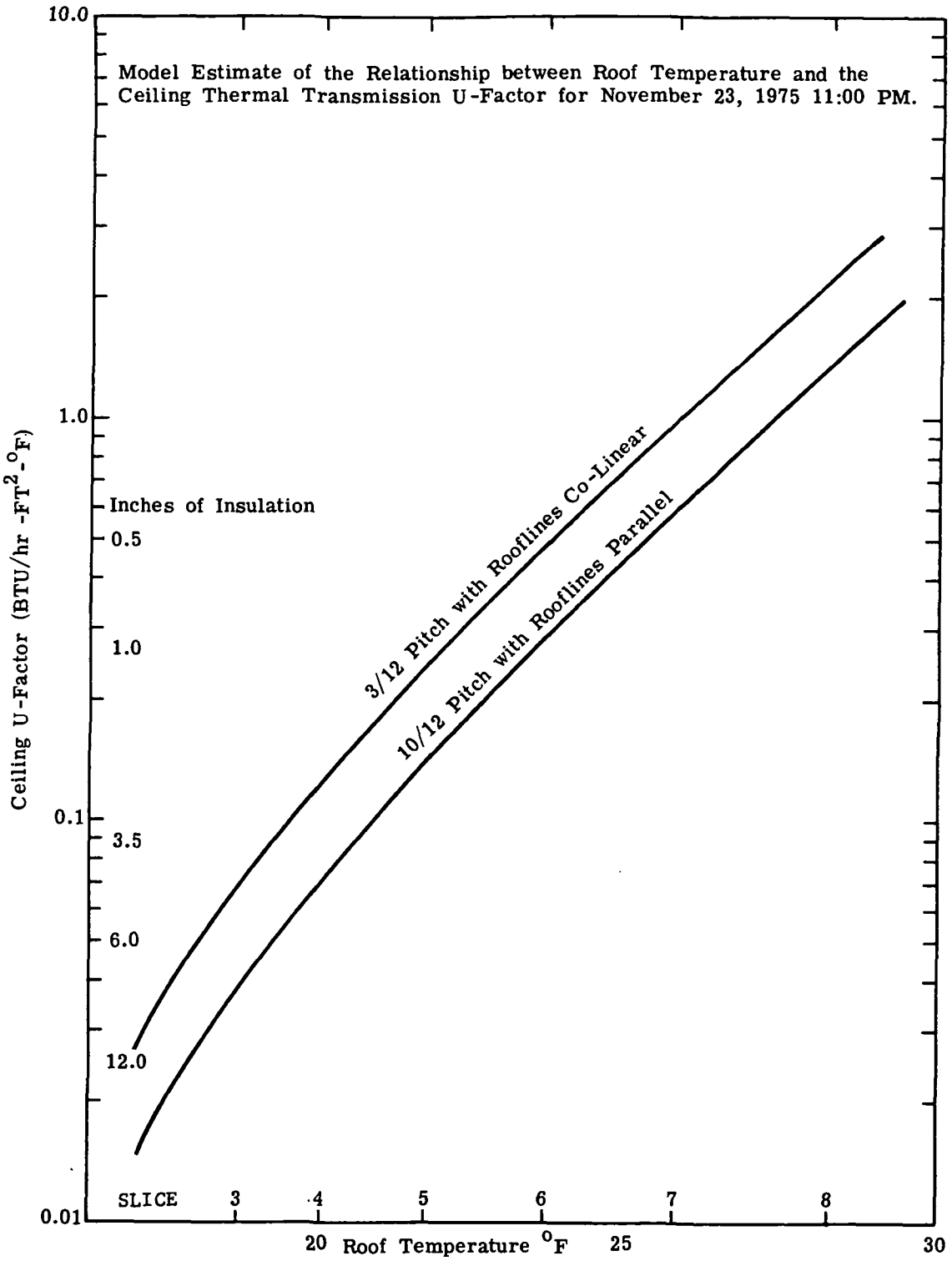
Model Estimate of the Relationship between Roof Temperature and the Ceiling Thermal Transmission U-Factor for November 23, 1975 11:00 PM.
Ceiling U-Factor (BTU/hr -FT^2-^{o}F)
10.0
1.0
0.1
0.01
Inches of Insulation
0.5
1.0
3.5
6.0
12.0
3/12 Pitch with Rooflines Co-Linear
10/12 Pitch with Rooflines Parallel
SLICE 3 4 5 6 7 8
20 Roof Temperature ^{o}F 25 30

FIGURE 4

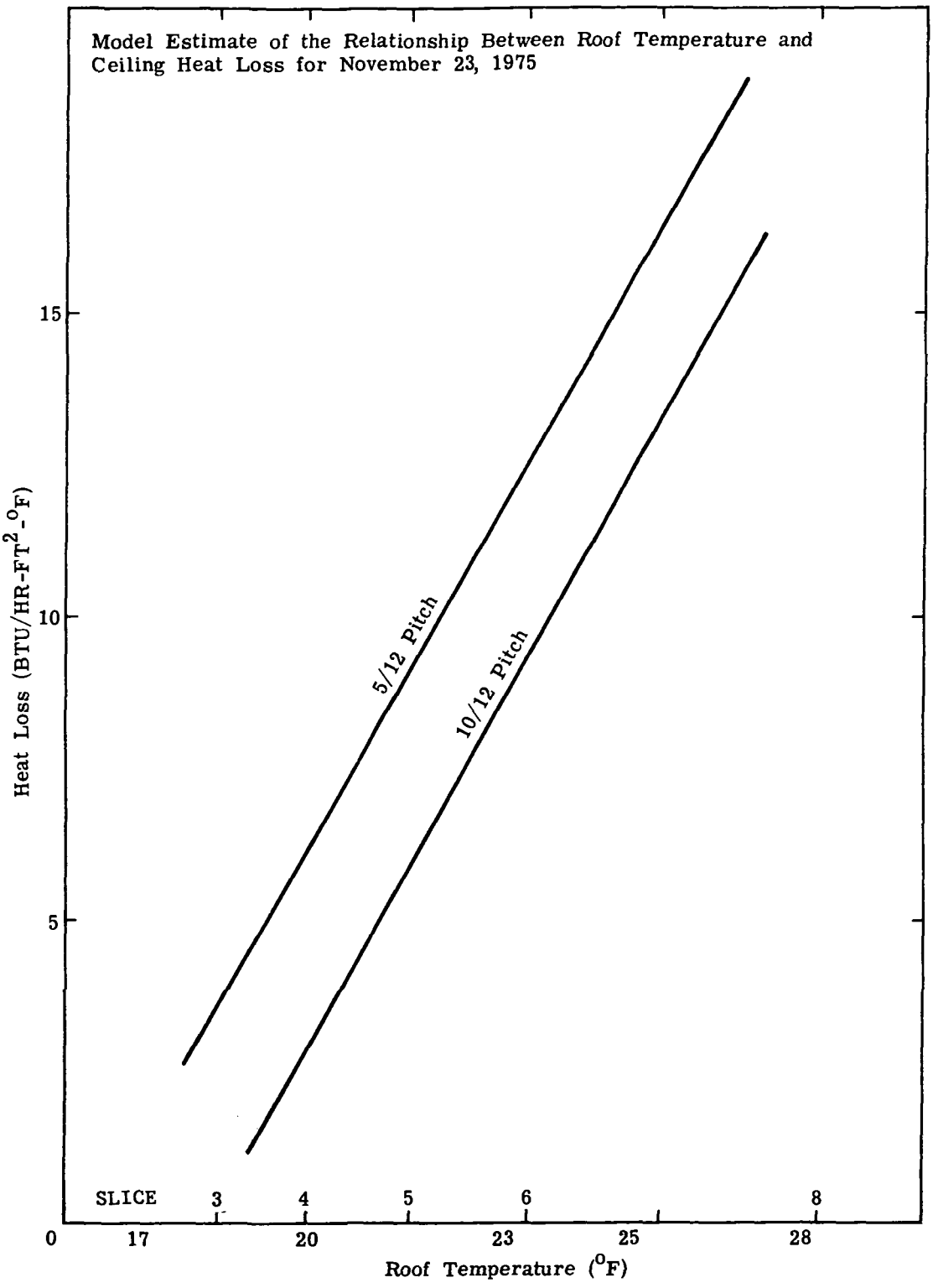
Model Estimate of the Relationship Between Roof Temperature and Ceiling Heat Loss for November 23, 1975
Heat Loss (BTU/HR-FT^2-^{o}F)
15
10
5
0
5/12 Pitch
10/12 Pitch
SLICE
3
4
5
6
8
17
20
23
25
28
Roof Temperature (^{o}F)

FIGURE 5

TABLE 1. SUMMARY OF SURVEY RESULTS

Temperature Level	Total Responses	Sub-Area 1	Sub-Area 2	Sub-Area 3	Sub-Area 4	Insulated*	Uninsulated	Ave. Report Insulation (in.)	Unknown	Average Gas Consumption KBTU/hr
3	19	1	13	4	1	14	0	4.9	5	30.4
4	48	26	18	4	1	39	0	5.25	9	28.5
5	55	20	6	6	23	43	3	3.0	9	32.0
6	83	10	0	13	59	43	19	3.3	21	35.4
7	51	11	0	2	38	16	16	2.4	19	48.4
Totals	256	68	37	29	122	155	38		63	
Average Natural Gas Consumption KBTU/hr		26.8	32.5	30.8	41.4					
Average Reported Insulation (in.)		4.6	5.0	3.9	3.4					

*Insulated Means Two or More Inches of Insulation Reported to be in the Ceiling.

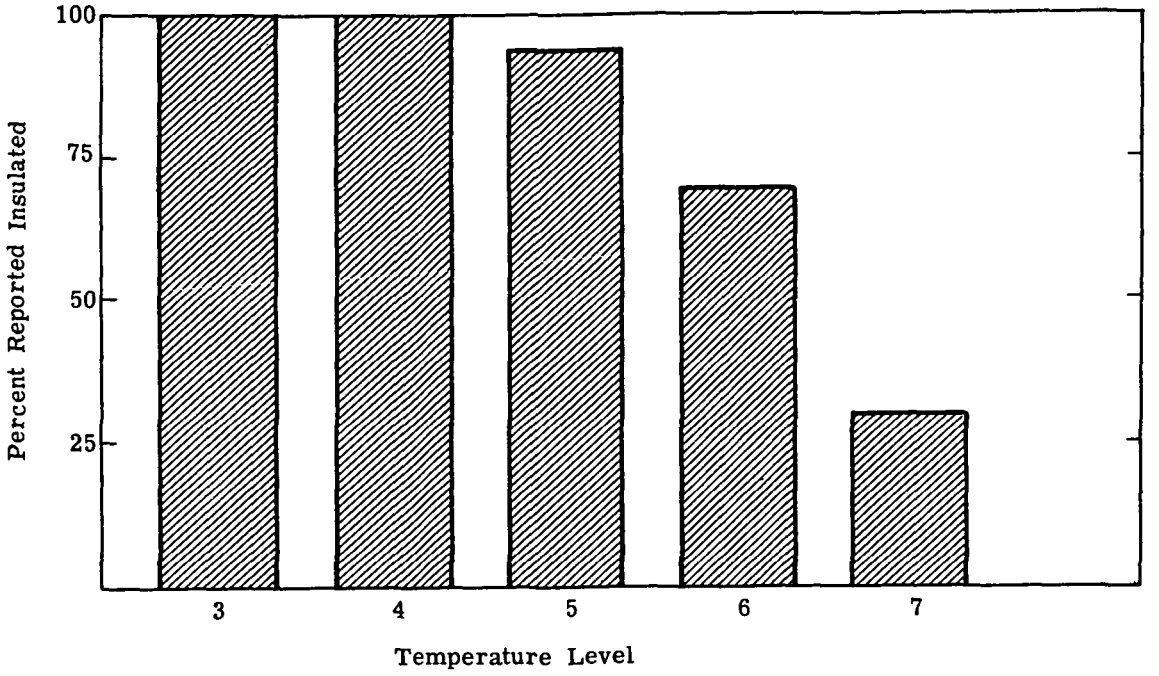

FIGURE 6. PERCENT CORRECT CLASSIFICATION OF REPORTED INSULATED AND UNINSULATED HOUSES USING ROOF TEMPERATURES OBTAINED FROM AERIAL IMAGERY.

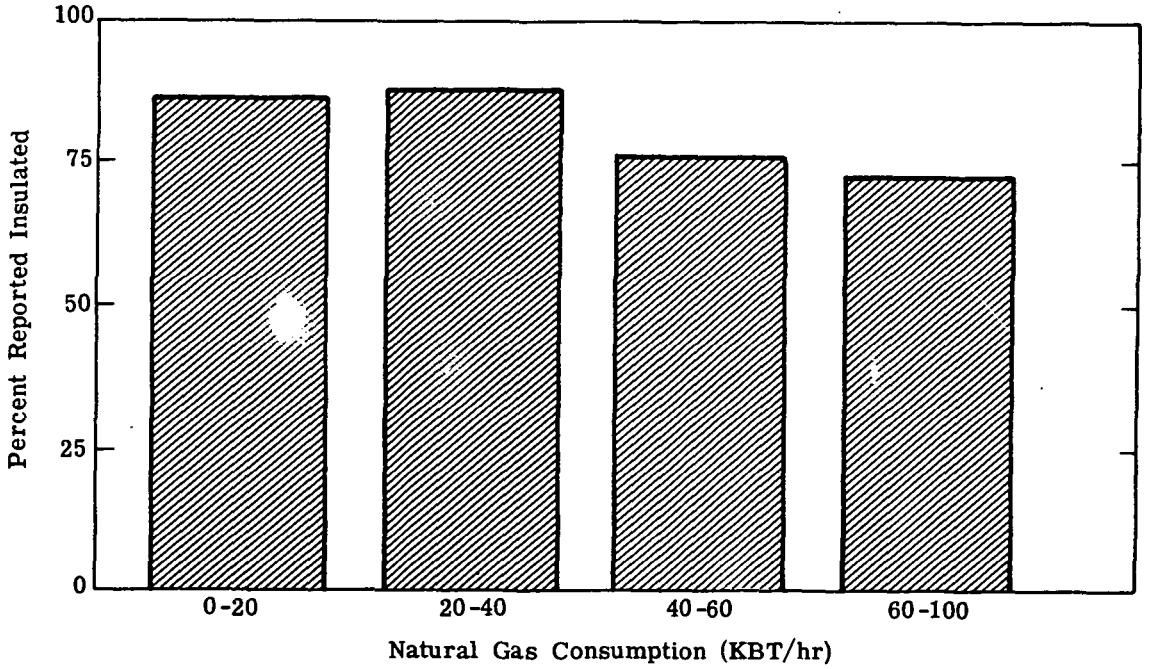

FIGURE 7. GAS CONSUMPTION VALUES WITH REPORTED INSULATION LEVELS.

consumption values to be nearly independent of the amount of insulation. Thus, gas consumption alone appears to offer little capability of discriminating insulated and non-insulated ceilings.

DISCUSSION

As applied to heat loss through building roofs this aerial infrared technique gives promising results but needs further evaluation work. Improvements in prediction capability may improve if finer temperature slices were used and more precise model parameters obtained. However, due to the uncertainty and difficulty in obtaining specific building parameter predictive capabilities of aerial thermography will be limited to a few general classes of insulation level. Causes for the incorrect interpretation include mistakes in the questionnaire response, variation in surroundings and emissivities, and variation in interior temperature and ceiling/roof construction. Further work is needed to more precisely estimate actual insulation thickness and remove the scatter in the results.

The aerial infrared technique can be applied to monitor heat loss of buildings over large metropolitan areas and to support large scale retrofit insulation programs.

REFERENCES

1. F.J. Tanis, R.E. Sampson, T.W. Wagner. Thermal Imagery for Evaluation of Construction and Insulation Conditions of Small Buildings, ERIM Report 116600-12-F, for Federal Energy Administration, July 1976.

2. J. Bjorklund, F.A. Schmer, and R.E. Isakson. Aerial Thermal Scanner Data for Monitoring Rooftop Temperature. Remote Sensing Institute, South Dakota State University, Brookings, South Dakota, November 1975.